



Lightning NO₂ simulation over the Contiguous US and its effects on satellite NO₂ retrievals

Qindan Zhu¹, Joshua L. Laughner^{2,*}, and Ronald C. Cohen^{1,2}

¹Department of Chemistry, University of California, Berkeley, Berkeley, CA 94720

²Department of Earth and Planetary Sciences, University of California, Berkeley, Berkeley, CA 94720

*Now in Department of Environmental Science and Engineering, California Institute of Technology, Pasadena, CA 91125

Correspondence to: Ronald C. Cohen (rccohen@berkeley.edu)

Abstract. Lightning is an important NO_x source representing ~10% of the global source of odd N and a much larger percentage in the upper troposphere. The poor understanding of spatial and temporal patterns of lightning contributes to a large uncertainty in understanding upper tropospheric chemistry. We implement a lightning parameterization using the product of convective available potential energy (CAPE) and convective precipitation rate (PR) into Weather Research and Forecasting-Chemistry (WRF-Chem) model for North America. We show that the CAPE-PR parameterization with a regional scaling factor of 0.5 in the southeastern US yields an improved representation of lightning flashes in WRF when comparing against flash density from the Earth Networks Total Lightning Network. Compared to the cloud top height (CTH) lightning parameterization used in WRF-Chem, simulated NO₂ profiles using the CAPE-PR parameterization exhibit better agreement with aircraft observations in the middle and upper troposphere. While the lightning NO_x production rate is 500 mol NO flash⁻¹, using the a priori NO₂ profile generated by the simulation with the CAPE-PR parameterization reduces the air mass factor for NO₂ retrievals by 16% on average in the southeastern US on the late spring and early summer; yielding an overall 20% enhancement of the NO₂ vertical column density compared to simulations using the CTH lightning parameterization.

1 Introduction

Nitrogen oxides (NO_x ≡ NO + NO₂) are key species in the atmosphere chemistry, affecting the oxidative capacity in the troposphere by regulating the ozone and hydroxyl radical concentrations (Crutzen, 1979). Anthropogenic sources (mainly fossil fuel combustion) are the largest contributor to the NO_x budget on a global scale. Natural sources of NO_x are also nonnegligible (Denman et al., 2007). While anthropogenic emissions of NO_x are intensively studied, natural sources are less understood (e.g. Delmas et al., 1997; Lamsal et al., 2011; Miyazaki et al., 2012). Lightning contributes to ~10% of NO_x budget on a global scale and represents over 80% of NO_x in the upper troposphere (UT) (Schumann and Huntrieser, 2007; Nault et al., 2017). Over the US, the anthropogenic NO_x emissions have been decreasing rapidly (Russell et al., 2012; Lu et al., 2015), making lightning an increasingly important source of NO_x and an increasingly large fraction of the source of column NO₂. Ozone (O₃) in UT has long lifetime and leads to a more pronounced radiative effect than ozone elsewhere in the troposphere. Varying lightning NO_x emission (LNO_x) by a factor of four (123 to 492 mol NO flash⁻¹) yields up to 60 % enhancement of UT O₃ and increases the mean net radiative flux by a factor of three (Liaskos et al., 2015). This range in the lightning NO_x



production rate is similar to the current uncertainty of estimated lightning emission rates. Further, incorrect representation of LNO_x in a priori profiles for satellite NO_2 retrievals leads to biases in the retrieved NO_2 columns. This is exacerbated by the greater sensitivity of UV/Vis NO_2 retrievals to the UT (e.g. Laughner and Cohen, 2017; Travis et al., 2016).

When lightning occurs, NO is emitted as a result of high temperatures and NO_2 forms through rapid photochemistry. Numerous studies report the estimated LNO_x production rate with ranges from 16 to 700 mol NO flash⁻¹ (DeCaria et al., 2005; Hudman et al., 2007; Martin et al., 2007; Schumann and Huntrieser, 2007; Huntrieser et al., 2009; Beirle et al., 2010; Bucsela et al., 2010; Jourdain et al., 2010; Ott et al., 2010; Miyazaki et al., 2014; Liaskos et al., 2015; Pickering et al., 2016; Pollack et al., 2016; Laughner and Cohen, 2017; Nault et al., 2017).

Two categories of methods, one emphasizing the near-field of lightning NO_x and the other the far-field, have previously been applied to estimate LNO_x . In near-field approaches the total NO_x from direct observation close to the lightning flashes is divided by the number of flashes from a lightning observation network to yield the NO_x per flash. In contrast, the far-field approach uses downwind observations to constrain a regional or global chemical transport model. The emission rate of lightning NO_x is varied in the model (either ad hoc or through formal assimilation methods) until the modeled NO_x agrees with the measurements of total NO_x at the far field location (Hudman et al., 2007; Martin et al., 2007; Jourdain et al., 2010; Miyazaki et al., 2014; Liaskos et al., 2015; Laughner and Cohen, 2017; Nault et al., 2017). In general, far-field approaches yield estimates of LNO_x at the upper end of reported range, while estimates from the near-field studies are typically at the lower end of the range. Nault et al. (2017) showed that a large part of this discrepancy is because prior near-field studies assume a long NO_x lifetime in the UT, while active peroxy radical chemistry in the near field leads to a short NO_x lifetime (~3 h). Without accounting for this chemical loss, the near-field estimates are biased low. However, this cannot completely reconcile the discrepancy between near- and far- field studies.

In chemical transport models, LNO_x production is modeled by assuming a fixed number of moles of NO are produced per lightning flash, typically 250 or 500 mol NO flash⁻¹ (Zhao et al., 2009; Allen et al., 2010; Ott et al., 2010). This presents an additional challenge to the far-field approaches to constrain LNO_x , as errors in the simulation of lightning flashrate will propagate into errors in the LNO_x production per flash. However, explicitly simulating the cloud scale processes that produce lightning is generally too computationally expensive to be applied in a regional model as it requires spatial resolution at the same scale of cloud processes. Instead, the convection is parameterized using simplified convection schemes. Lightning is then parameterized by a suite of convection parameters. The most prevalent lightning parameterization relates lightning to the cloud top height (CTH) (Price and Rind, 1992; Price et al., 1997). Price and Rind found a consistent proportionality between cloud-to-ground (CG) lightning flashes and the fifth power of cloud top height. Other meteorological variables, including upward cloud mass flux (UMF), convective precipitation rate (CPR), convective available potential energy (CAPE), cloud ice flux (ICEFLUX) have been suggested as alternative lightning proxies for CG flashes or in some cases total flashes (Allen and Pickering, 2002; Choi et al., 2005; Wong et al., 2013; Romps et al., 2014; Finney et al., 2014). When CG flashes are predicted, the total lightning rate, including CG and Intra-Cloud (IC) flashes, is derived by defining a regional dependent CG:IC ratio (Boccippio et al., 2002).



Several previous studies have evaluated the performance of these lightning parameterizations in regional and global models. Tost et al. (2007) concluded none of them accurately reproduce the observed lightning observations even though some are inter-comparable. Wong et al. (2013) showed that a model using the CTH lightning parameterization simulates erroneous flash count frequency distribution while the integrated lightning flash count is consistent with the observation. Luo et al. (2017) tested the single-variable parameterizations (CTH, CAPE, UMF, CPR) and the paired parameterizations based on power law relationship (CAPE-CTH, CAPE-UMF, UMF-CTH), and demonstrated that two-variable parameterization using CAPE-CTH improves upon the previous single-variable parameterizations; it captures temporal change of flash rates but the simulated spatial distribution is still not satisfactory.

In this study, we implemented the CAPE-PR lightning parameterization into WRF-Chem and assess the performance in reproducing lightning flash density. Our motivation is to produce a better representation of a proxy-based lightning parameterization in the regional chemistry transport model. We also evaluate the effect of modeled lightning NO_x on both the a priori profiles used in satellite NO_2 retrievals and the retrievals themselves.

2 Methods: models and observations

2.1 WRF-Chem

This study employs the Weather Research and Forecast Model coupled with Chemistry (WRF-Chem) version 3.5.1. The model domain covers North America from 20°N to 50°N with $12\text{ km} \times 12\text{ km}$ horizontal resolution and 29 vertical layers. The North American Regional Reanalysis (NARR) provides initial and boundary conditions. Temperature, wind direction, wind speed and water vapor are nudged every 3 h towards to NARR product. Chemistry initial and boundary conditions are provided by the Model for Ozone and Related Chemistry Tracers (MOZART, <https://www.acom.ucar.edu/wrf-chem/mozart.shtml>). Anthropogenic emissions are driven by the National Emissions Inventory 2011 (NEI 11), with a scaling factor to match the total emissions to 2012 emission from the Environmental Protection Agency (EPA, 2016). Biogenic emission are driven by the Model of Emissions of Gases and Aerosol from Nature (MEGAN; (Guenther et al., 2006)). We use a customized version of the Regional Atmospheric Chemistry Mechanism version 2 (RACM2), the details are described by Zare et al. (2018).

The default lightning parameterization used in WRF-Chem is based on cloud top height (CTH). The parameterized lightning flash rates are proportional to a power of cloud top height with linear scaling varied by region:

$$f = \begin{cases} 3.44 \times 10^{-5} H^{4.9} & \text{Continental} \\ 6.20 \times 10^{-4} H^{1.73} & \text{Marine} \end{cases} \quad (1)$$

where f is the CG flash rate in each grid and H is the colocated cloud top height in units of kilometers.



We also implement an alternative lightning parameterization where lightning flash rates are defined to be proportional to the product of the convective available potential energy (CAPE) and precipitation rate (PR).

$$f = \begin{cases} 0.9 \times 10^{-4} \times E \times PR & \text{Southeastern CONUS} \\ 1.8 \times 10^{-4} \times E \times PR & \text{Elsewhere CONUS} \end{cases} \quad (2)$$

where f the CG flash rate in each grid cell, E the convective available potential energy and PR the convective precipitation rate. Southeastern CONUS in the context is the region between 94 °W to 76 °W and 25 °N to 37 °N. This parameterization was proposed by Romps et al. (2014). Romps et al. (2014) used a year-round observation of lightning and meteorological parameters and found a good correlation between observed lightning flash densities and observed CAPE times PR over the CONUS. CAPE-PR was further examined in Tippett and Koshak (2018) who computed the proxy in a numerical forecast model and found a fairly good agreement between the spatial pattern of the daily CG flash rate and the forecast proxy over 2003-2016. To our knowledge CAPE-PR parameterization has not previously been coupled with chemistry. Note that we compute these two meteorological variables every 72 seconds in our model setup and produce lightning flash rates in a much shorter time step compared to Romps et al. (2014) and Tippett and Koshak (2018). We also apply a regional scaling factor of 0.5 to the southeastern US (See Sec 3.1).

We analyze WRF-Chem outputs from two model runs. The first run is consistent with Laughner and Cohen (2017); it selects the Grell 3D ensemble cumulus convective scheme (Grell, 1993; Grell and Dévényi, 2002) and the CTH lightning parameterization. Grell 3D convective scheme readily computes natural buoyancy level which serves as the optimal proxy for cloud top height (Wong et al., 2013). The second run selects the Kain-Fritsch cumulus convective scheme (Kain and Fritsch, 1990; Kain, 2004) and the CAPE-PR lightning parameterization described above. Compared to the Grell 3D convective scheme, the Kain-Fritsch uses the depletion of at least 90% CAPE as the closure assumption and calculates CAPE on the basis of entraining parcels instead of undiluted parcels, which also improves the calculation of precipitation rate (Kain, 2004). Both runs define the lightning NO_x production rate to be 500 mol NO flash⁻¹. The CG:IC ratio and LNO_x post-convection vertical distribution are the same as Laughner and Cohen (2017).

2.2 ENTLN lightning observation network

To assess the performance of the lightning parameterizations we compare to lightning flashes from Earth Networks Total Lightning Network (ENTLN). ENTLN employs over 100 sensors across the United States and observes both CG and IC pulses (<https://www.earthnetworks.com/why-us/networks/lightning/>). All lightning pulses within 10 km and 700 ms of each other are grouped as a single flash. The IC and CG flashes are summed over the grid spacing defined in WRF-Chem. Among multiple lightning observation networks, ENTLN is selected for better coverage over the CONUS domain and for its high detection efficiency (~70%) (Rudlosky, 2015). Comparison between the ENTLN and the Tropical Rainfall Measurement Mission (TRMM) Lightning Imaging Sensor (LIS) yields a broad agreement during the time period covered in this study, as shown in Fig. S1.



		CTH	CAPE-PR
Southeastern	Slope	2.08	0.98
	R^2	0.30	0.72
Elsewhere	Slope	0.98	1.19
	R^2	0.27	0.62

Table 1. Correlation statistics between observed and modeled (CTH, CAPE-PR) flash density per day averaged by regions

2.3 In Situ Aircraft Measurements

We compare our simulations to observations from aircraft campaigns that focus on deep convection. The Deep Convective Clouds and Chemistry (DC3) campaign (Barth et al., 2015) took place during May and June of 2012 over Colorado, Oklahoma, Texas and Alabama. The Studies of Emissions and Atmospheric Composition, Clouds, and Climate Coupling by Regional Surveys (SEAC4RS) (Toon et al., 2016) took place during August and September of 2013; most of the flight tracks occurred over the southeastern US. Both aircraft campaigns flew into and out of storms and sampled deep convection. The combination of these two aircraft campaigns cover the regions with the most active lightning in the domain.

2.4 Satellite Measurements

The Ozone Monitoring Instrument is an ultraviolet/visible (UV/Vis) nadir solar backscatter spectrometer launched in July 2004 on board the Aura satellite. It detects backscattered radiance in the range of 270-500 nm and the spectra are used to derive column NO_2 at a spatial resolution of $13 \text{ km} \times 24 \text{ km}$ at nadir (Levelt et al., 2006).

We use the Berkeley High Resolution (BEHR) v3.0B OMI NO_2 retrieval (Laughner et al., 2018). The AMF is calculated based on the high spatial resolution a priori input data including surface reflectance, surface elevation and NO_2 vertical profiles. In this study we apply an experimental branch of the BEHR product which differs from v3.0B in several ways. First, the tropopause pressure is switched to NASA tropopause pressure instead of calculation based on temperature profiles from WRF-Chem (Mak et al., 2018). Analysis shows the algorithm used in BEHR v3.0B to calculate the WRF-derived tropopause pressure is very much dependent on the vertical spacing predefined in WRF-Chem setup, which causes biases when the vertical layers are at a coarse resolution. Second, the NO_2 vertical profiles are outputs using the modified lightning parameterization described in Eq. 2.

3 Results

3.1 Comparison with observed lightning flash density

The lightning parameterizations are compared against observations from ENTLN in Fig 1. Each of datasets is averaged from May 13 to June 23, 2012. The ENTLN data is summed to the $12 \text{ km} \times 12 \text{ km}$ WRF grid. The CTH parameterization fails to

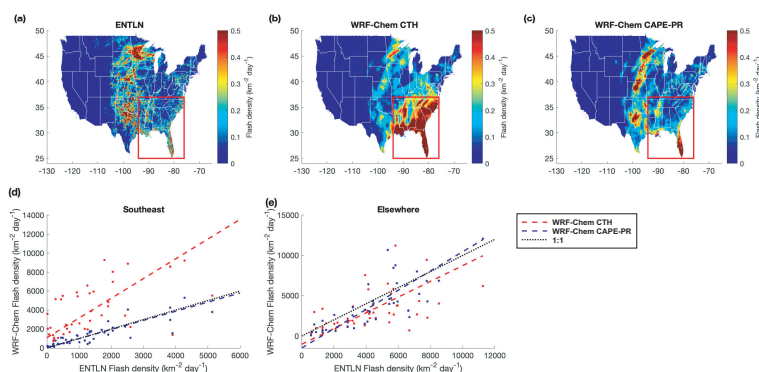


Figure 1. Observed flash densities from the ENTLN dataset (a) and WRF-Chem using two lightning parameterization, the CTH lightning parameterization (b) and the CAPE-PR lightning parameterization (c), respectively. The correlation of total flash density per day between WRF-Chem outputs and ENTLN for the southeastern US (denoted by the red box in a and b) is shown in panel (d) and the correlation for elsewhere in CONUS is shown in (e). The model using CTH is in red and the model using CAPE-PR is in blue. Dash lines are corresponding fits.

reproduce the spatial pattern of flashes observed by ENTLN over the CONUS. In contrast, the CAPE-PR parameterization better captures the spatial distribution of flash densities. However the CAPE-PR parameterization still fails to capture the gradients in flash occurrence within smaller regions. For instance, ENTLN shows that more lightning occurs along the east coast than west coast in Florida, however, WRF-Chem generates a lightning flash density of the same magnitude over both areas. Nevertheless, the CAPE-PR substantially improves the model performance in reproducing lightning spatial patterns.

To evaluate the agreement quantitatively, we regress the WRF daily regional average flash densities against those measured by ENTLN. The daily regional averaged flash density is calculated by summing the total flash rates and dividing them by the corresponding regional size. The regressions are shown in Fig 1 (d) and (e); the correlation statistics are shown in Table 1. The model using the CAPE-PR lightning parameterization yields a tight correlation and slope close to the unity over the US domain. In the southeastern US, the R^2 increases from 0.3 to 0.7 and slope is reduced from 2.08 to 0.96 with the CAPE-PR parameterization compared to CTH. Note that the improved scaling of the slope is mainly caused by the scaling factor of 0.5 applied to the southeast region. In this simulation, a constant linear coefficient for CAPE-PR is not adequate to represent the observed lightning over CONUS, in contrast to the finding of Romps et al. (2014). Elsewhere in CONUS, the R^2 improves from 0.3 to 0.6 with slopes increasing by 20%. In general the CAPE-PR lightning parameterization captures the day-to-day variation in flash densities better than the CTH parameterization.

3.2 Comparison with observed vertical profiles

We compare the WRF NO_2 profile to the average vertical profile of NO_2 measured during DC3 and SEAC4RS in Fig 2. Data points are matched in time and space by finding the WRF-Chem output nearest in time and closest in space to a given

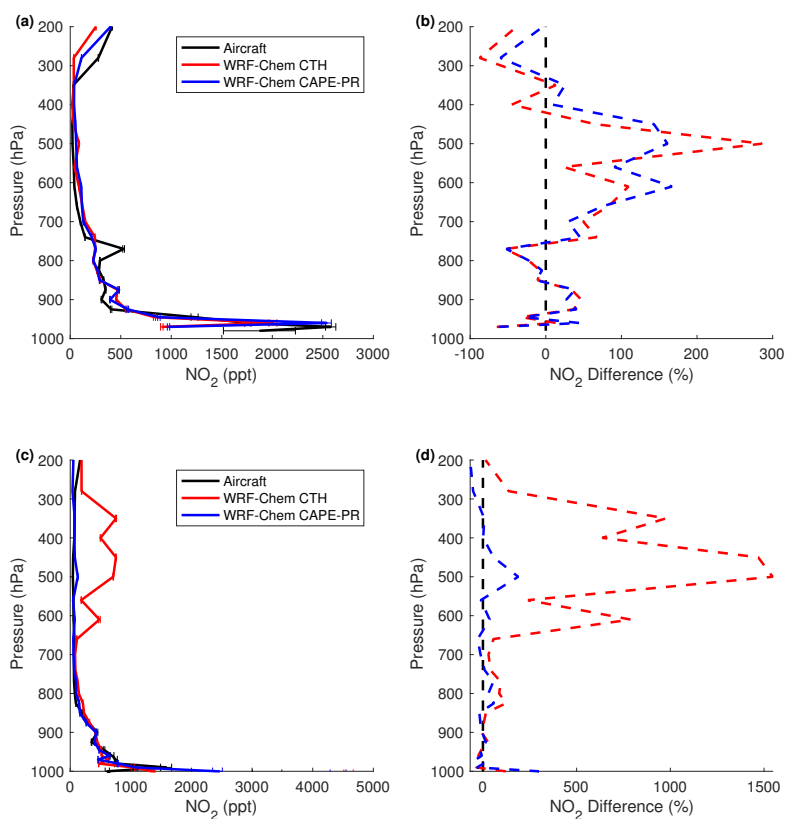


Figure 2. Comparison of WRF-Chem and aircraft NO_2 profiles from the (a,b) DC3, (c,d) SEAC4RS campaigns. Vertical NO_2 profiles are shown in (a,c), the solid line is the mean of all profiles and the bars are 1 standard deviation for each binned level. The corresponding relative difference compared to observations are shown in (b,d). Aircraft measurements are shown in black, WRF-Chem using CTH lightning parameterization in red and WRF-Chem using CAPE-PR lightning parameterization in blue.

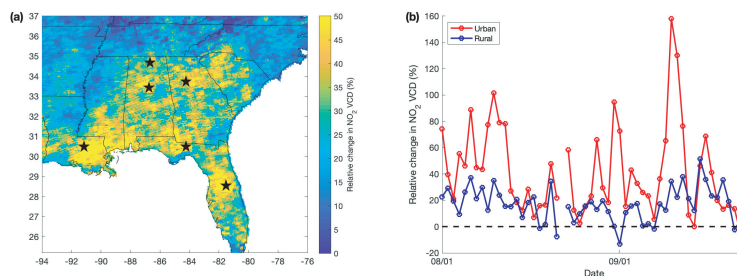


Figure 3. Relative change in BEHR NO_2 VCD over the southeastern US switching the source of a prior NO_2 profiles from WRF-chem outputs using CTH to one using CAPE-PR lightning parameterization. (a) shows the mean spatial distribution of the changes from Aug 01 to Sep 23, 2013 and (b) shows the temporal variation over urban and rural areas. Medium to large cities, including Atlanta, GA; Huntsville, AL; Birmingham, AL; Tallahassee, FL; Orlando, FL; and Boton Rouge, LA, are marked by stars in panel (a).

		AMF CTH	AMF CAPE-PR	% Δ AMF	VCD CTH	VCD CAPE-PR	% Δ VCD
Aug 31	Urban	1.71	0.55	-67.9	2.01×10^{15}	6.48×10^{15}	222.2
	Rural	2.88	1.89	-34.4	1.05×10^{15}	1.38×10^{15}	34.4
Sep 14	Urban	0.74	0.75	1.5	5.59×10^{15}	3.92×10^{15}	-1.8
	Rural	0.82	0.86	4.8	2.24×10^{15}	2.13×10^{15}	-4.8

Table 2. Differences for BEHR AMFs and tropospheric VCDs when using the a priori NO_2 profiles from models with CTH vs CAPE-PR parameterizations in the AMF calculation. For definitions of “urban” and “rural”, see the text.

observation. The effect of lightning NO_x is indistinguishable close to the surface. In the upper and middle troposphere, both model simulations yields similar NO_2 vertical profiles compared to the measurements from DC3. WRF-Chem using CAPE-PR performs better comparing NO_2 profile between 200 hPa to 400 hPa but the negative bias still exists. The largest percentage difference occurs in the middle troposphere between 400 hPa to 700 hPa where observations cannot capture NO_2 but the model predicts an appreciable amount of NO_2 compared to observations.

Laughner et al. (2019) previously identified a high bias of WRF-Chem UT NO_2 versus SEAC4RS in the southeast US when using the CTH parameterization. The model using the CAPE-PR parameterization reduces this high bias of NO_2 in the middle and upper troposphere. The CAPE-PR parameterization slightly overestimates it NO_2 in the middle troposphere (400 - 530 hPa) and underestimates in the upper troposphere (< 280 hPa), which is consistent with the comparison to observations from DC3 campaign.

3.3 Impact on BEHR NO_2 retrievals

In space-based retrievals of NO_2 , an air mass factor (AMF) is required to convert the slant column density (SCD) obtained by fitting the observed radiances into a vertical column density (VCD). The AMF depends on scattering weights (which describe the sensitivity of the measurement to different levels of the atmosphere) and an NO_2 profile simulated by a chemical transport



model, such as WRF-chem. Over a dark surface, the scattering weights in the UT are up to 10x greater than near the surface, due to the greater probability that a photon that reaches the lower troposphere will be absorbed by the surface. Therefore, errors in the UT NO_2 profile can have large effects on the AMF (e.g. Laughner and Cohen, 2017). Here, we investigate how the NO_2 profiles simulated by the CAPE-PR parameterization affect the BEHR NO_2 retrievals.

5 Fig. 3(a) shows the relative change in tropospheric VCD averaged between Aug 01 to Sep 23, 2013 induced by changing the a priori profiles from the model using CTH to the one using the CAPE-PR lightning parameterization. The relative enhancement of VCD is 19% on average over southeast US but it varies significantly.

The spatial pattern in Fig. 3(a) suggests that the magnitude of the improved representation of lightning is quite different in urban and rural areas. The cities indicated by stars and their vicinity regions are associated with substantial increase in NO_2 VCD. To quantify this, we define urban and rural areas by difference in column NO_2 . We calculate VCDs using AMFs
10 computed with a priori profiles from a simulation without LNO_x and select the 5% and 95% percentiles of NO_2 VCD as thresholds. Urban areas are the top 5% of columns and rural areas the bottom 5%, respectively. Fig 3(b) shows the relative change in VCD over the urban and rural areas as a function of time. The increase in VCD due to the change in profiles is more pronounced over urban areas with averaged relative change of ~60% compared to the average change of ~25% in rural areas.
15 Changes in urban VCDs span 0 to 220%. In contrast, using the NO_2 profiles produced by the CAPE-PR simulation leads to only maximum 51.2% increase in VCD over rural areas.

Table 2 presents the AMF and VCD obtained from using a priori profiles with CTH or CAPE-PR lightning parameterizations as well as the relative changes on Aug 31 and Sep 14, 2013. Aug 31 is an example of one day when the change in NO_2 profiles has a very large impact on the NO_2 VCDs. The VCD increases by 222% over urban areas and 34% over rural
20 areas; the corresponding change in AMF is 68% and 34%, respectively. In contrast, Sep 14 is an example where the lightning parameterization has very little effect. The relative change in VCD is -1.8% over urban areas and -4.8% over rural areas.

4 Discussion

Here, we apply the improved CAPE-PR simulation to the problem of constraining LNO_x production over CONUS. To do so, we vary the lightning NO_x production rate prescribed in WRF-Chem to produce the simulated map of NO_2 VCD, and
25 compare against OMI NO_2 retrievals using a priori profiles from model simulations with the same LNO_x production rate. In our model-satellite comparisons the averaging kernel is applied to remove the representative errors introduced by a priori knowledges of NO_2 vertical profiles (Boersma et al., 2016). Figure 4 (a, b), Fig. S2 and Fig. S3 show that the lightning NO_x production rate of 500 mol NO flash⁻¹ yields the lowest root-mean-square error (RMSE) between modeled and observed NO_2 VCD, which is at the high end of previous estimates of the lightning NO_x production rate (16-700 mol NO flash⁻¹).

30 However, we note that this lightning NO_x estimate is systematically biased high due to the negative bias in $[\text{NO}_2]/[\text{NO}_x]$ ratio in the middle and upper troposphere. The satellite observed NO_2 column serves as a proxy for total NO_x emitted by lightning. The rapid interconversion between NO and NO_2 reaches the photochemical steady state in a short time (~120s). Consequently, if the model kinetics result in an incorrect NO - NO_2 photochemical steady state ratio, this error will propagate

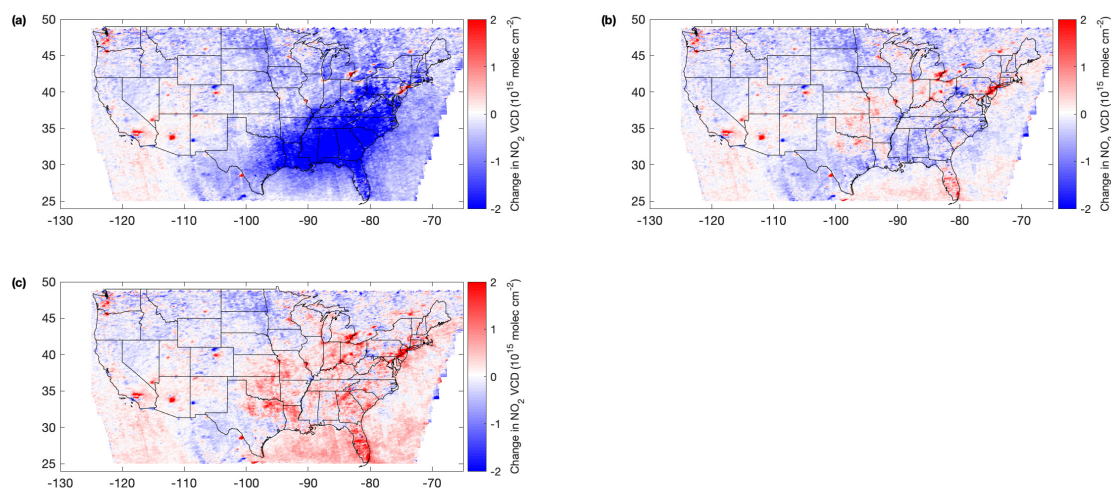


Figure 4. Difference in NO_2 VCD between BEHR retrievals and WRF-Chem. (a) excludes LNO_x in model simulation, (b) adds LNO_x emission with production rate of $500 \text{ mol NO flash}^{-1}$. (c) includes the same LNO_x emission as (b) but uses NO_2 profiles scaled up by 60% at pressure lower than 400 hPa.

into the LNO_x production estimate. Comparisons against aircraft measurements show $[\text{NO}_2]/[\text{NO}_x]$ ratio in the WRF-Chem simulations is around 40% smaller than observations in upper troposphere (Fig. S4). Given that the simulated $[\text{NO}_2]/[\text{NO}_x]$ is too small, the model will simulate smaller NO_2 VCDs per unit of LNO_x emitted, requiring a greater LNO_x production efficiency to match satellite NO_2 VCD observations. Modeled NO_2 columns are recalculated with NO_2 profiles scaled up by 60% (the ratio of observed and modeled $[\text{NO}_2]/[\text{NO}_x]$) at pressure levels where $p < 400 \text{ hPa}$, and the comparison between revised model and observation is shown in Fig. 4 (c). This suggests that the $500 \text{ mol NO flash}^{-1}$ is greater than the actual LNO_x production rate when the bias caused by $[\text{NO}_2]/[\text{NO}_x]$ ratio is accounted for.

Several recent studies also report an underestimate in modeled $[\text{NO}_2]/[\text{NO}_x]$ ratios in SE US (Travis et al., 2016; Silvern et al., 2018); both feature observations from SEAC4RS field campaign to validate model simulations. Silvern et al. (2018) suggests the underestimate is either caused by an unknown labile NO_x reservoir species or error in reaction rate constant for the $\text{NO} + \text{O}_3$ reaction and NO_2 photolysis reaction. In contrast, Nault et al. (2017) utilizes measurements from DC3 field campaign and demonstrates a positive bias in modeled $[\text{NO}_2]/[\text{NO}_x]$ ratio compared against observations. Understanding the difference in $[\text{NO}_2]/[\text{NO}_x]$ between model and observations requires additional study, but is crucial to reducing the uncertainty in LNO_x estimates.



5 Conclusions

We implement an alternative lightning parameterization based on convective available potential energy and precipitation rate into WRF-Chem and evaluate its performance in simulating lightning NO_x . We first validate it by comparing against lightning observations and conclude that the CAPE-PR parameterization with a regional scaling factor of 0.5 in the southeastern US improves the model representation of spatial pattern and day-to-day variation of lightning flashes. We also compare the simulated NO_2 profiles against aircraft measurements and find that the simulated NO_2 is more consistent with observations in the mid and upper troposphere.

The improved lightning NO_2 simulation has significant impact on AMFs and VCD of NO_2 . Over the southeastern US the AMF is reduced by 16% on average leading to a 19% increase in the NO_2 VCD. The effects on AMF and on VCD are very locally dependent. The VCD increase over urban areas is more pronounced and can be up to over 100%. This study emphasizes the importance of including reliable lightning NO_2 in a priori profiles for satellite retrievals.

The model-satellite NO_2 column comparison suggests 500 mol NO flash⁻¹ is too high for the estimate of lightning NO_x production rate, but demonstrate that the uncertainty in the modeled UT $[\text{NO}_2]/[\text{NO}_x]$ ratio is a key limiting factor in constraining production efficiency over CONUS in the far-field approaches.

15 *Data availability.* The experimental branch of BEHR v3.0B product used in this study is hosted by UC Dash (Zhu et al., 2019a, b) as well as on behr.cchem.berkeley.edu. The BEHR algorithm is available at <https://github.com/CohenBerkeleyLab/BEHR-core/> (Laughner and Zhu, 2018). The revised WRF-Chem code is available at <https://github.com/CohenBerkeleyLab/WRF-Chem-R2SMH/tree/lightning> (Zhu and Laughner, 2019).

Author contributions. RCC directed the research topic and QZ, JLL and RCC designed this study; JLL and QZ developed BEHR products; **20** QZ performed the analysis and prepared the manuscript with contributions from JLL and RCC. All authors have reviewed and edited the paper.

Competing interests. The authors declare no competing interests.

Acknowledgements. This work was supported by a NASA ESS Fellowship NNX14AK89H (Laughner), NASA grants NNX15AE37G and 80NSSC18K0624, and the TEMPO project SV3-83019. We acknowledge use of the Savio computational cluster resource provided by the **25** Berkeley Research Computing program at UC Berkeley which is supported by the UC Berkeley Chancellor, Vice Chancellor for Research, and Chief Information Officer. We thank Earth Networks Company for providing the Earth Networks Total Lightning Network (ENTLN)



datasets. We appreciate use of the WRF-Chem preprocessor tool (mozbc) provided by the Atmospheric Chemistry Observations and Modeling Lab (ACOM) of NCAR and use of MOZART-4 global model output available at <http://www.acom.ucar.edu/wrfchem/mozart.shtml>.



References

- Allen, D., Pickering, K., Duncan, B., and Damon, M.: Impact of lightning NO emissions on North American photochemistry as determined using the Global Modeling Initiative (GMI) model, *Journal of Geophysical Research: Atmospheres*, 115, <https://doi.org/10.1029/2010JD014062>, <https://agupubs.onlinelibrary.wiley.com/doi/abs/10.1029/2010JD014062>, 2010.
- 5 Allen, D. J. and Pickering, K. E.: Evaluation of lightning flash rate parameterizations for use in a global chemical transport model, *J. Geophys. Res. Atmos.*, 107, ACH 15–1–ACH 15–21, <https://doi.org/10.1029/2002JD002066>, <https://agupubs.onlinelibrary.wiley.com/doi/abs/10.1029/2002JD002066>, 2002.
- Barth, M. C., Cantrell, C. A., Brune, W. H., Rutledge, S. A., Crawford, J. H., Huntrieser, H., Carey, L. D., MacGorman, D., Weisman, M., Pickering, K. E., Bruning, E., Anderson, B., Apel, E., Biggerstaff, M., Campos, T., Campuzano-Jost, P., Cohen, R., Crouse, J., Day, D. A.,
10 Diskin, G., Flocke, F., Fried, A., Garland, C., Heikes, B., Honomichl, S., Hornbrook, R., Huey, L. G., Jimenez, J. L., Lang, T., Lichtenstern, M., Mikoviny, T., Nault, B., O'Sullivan, D., Pan, L. L., Peischl, J., Pollack, I., Richter, D., Riemer, D., Ryerson, T., Schlager, H., St. Clair, J., Walega, J., Weibring, P., Weinheimer, A., Wennberg, P., Wisthaler, A., Wooldridge, P. J., and Ziegler, C.: The Deep Convective Clouds and Chemistry (DC3) Field Campaign, *Bulletin of the American Meteorological Society*, 96, 1281–1309, <https://doi.org/10.1175/BAMS-D-13-00290.1>, <https://doi.org/10.1175/BAMS-D-13-00290.1>, 2015.
- 15 Beirle, S., Huntrieser, H., and Wagner, T.: Direct satellite observations of lightning-produced NO_x, *Atmos. Chem. Phys.*, 10, 10965–10986, <https://doi.org/10.5194/acp-10-10965-2010>, 2010.
- Boccippio, D. J., Koshak, W. J., and Blakeslee, R. J.: Performance Assessment of the Optical Transient Detector and Lightning Imaging Sensor. Part I: Predicted Diurnal Variability, *Journal of Atmospheric and Oceanic Technology*, 19, 1318–1332, [https://doi.org/10.1175/1520-0426\(2002\)019<1318:PAOTOT>2.0.CO;2](https://doi.org/10.1175/1520-0426(2002)019<1318:PAOTOT>2.0.CO;2), [https://doi.org/10.1175/1520-0426\(2002\)019<1318:PAOTOT>2.0.CO;2](https://doi.org/10.1175/1520-0426(2002)019<1318:PAOTOT>2.0.CO;2), 2002.
- 20 Boersma, K. F., Vinken, G. C. M., and Eskes, H. J.: Representativeness errors in comparing chemistry transport and chemistry climate models with satellite UV–Vis tropospheric column retrievals, *Geoscientific Model Development*, 9, 875–898, <https://doi.org/10.5194/gmd-9-875-2016>, <https://www.geosci-model-dev.net/9/875/2016/>, 2016.
- Bucsela, E. J., Pickering, K. E., Huntemann, T. L., Cohen, R. C., Perring, A., Gleason, J. F., Blakeslee, R. J., Albrecht, R. I., Holzworth,
25 R., Cipriani, J. P., Vargas-Navarro, D., Mora-Segura, I., Pacheco-Hernández, A., and Laporte-Molina, S.: Lightning-generated NO_x seen by the Ozone Monitoring Instrument during NASA's Tropical Composition, Cloud and Climate Coupling Experiment (TC4), *Journal of Geophysical Research: Atmospheres*, 115, n/a–n/a, <https://doi.org/10.1029/2009JD013118>, <http://dx.doi.org/10.1029/2009JD013118>, d00J10, 2010.
- Choi, Y., Wang, Y., Zeng, T., Martin, R. V., Kurosu, T. P., and Chance, K.: Evidence of lightning NO_x and convective transport of pollutants
30 in satellite observations over North America, *Geophysical Research Letters*, 32, <https://doi.org/10.1029/2004GL021436>, <https://agupubs.onlinelibrary.wiley.com/doi/abs/10.1029/2004GL021436>, 2005.
- Crutzen, P. J.: The Role of NO and NO₂ in the Chemistry of the Troposphere and Stratosphere, *Annual Review of Earth and Planetary Sciences*, 7, 443–472, <https://doi.org/10.1146/annurev.ea.07.050179.002303>, <https://doi.org/10.1146/annurev.ea.07.050179.002303>, 1979.
- DeCaria, A. J., Pickering, K. E., Stenchikov, G. L., and Ott, L. E.: Lightning-generated NO_x and its impact on tropospheric ozone production: A three-dimensional modeling study of a Stratosphere-Troposphere Experiment: Radiation, Aerosols and Ozone (STRAO-A)
35 thunderstorm, *Journal of Geophysical Research: Atmospheres*, 110, <https://doi.org/10.1029/2004JD005556>, <https://agupubs.onlinelibrary.wiley.com/doi/abs/10.1029/2004JD005556>, 2005.



- Delmas, R., Serça, D., and Jambert, C.: Global inventory of NO_x sources, *Nutrient Cycling in Agroecosystems*, 48, 51–60, <https://doi.org/10.1023/A:1009793806086>, <https://doi.org/10.1023/A:1009793806086>, 1997.
- Denman, K. L., Chidthaisong, A., Ciais, P., Cox, P. M., Dickinson, R. E., Hauglustaine, D., Heinze, C., Holland, E., Lohmann, U., Rameshchandran, S., et al.: Couplings between changes in the climate system and biogeochemistry, *International Panel on Climate Change*, pp. 499–587, 2007.
- EPA: Air Pollutant Emissions Trends Data, <https://www.epa.gov/air-emissions-inventories/air-pollutant-emissions-trends-data>, 2016.
- Finney, D. L., Doherty, R. M., Wild, O., Huntrieser, H., Pumphrey, H. C., and Blyth, A. M.: Using cloud ice flux to parametrise large-scale lightning, *Atmospheric Chemistry and Physics*, 14, 12 665–12 682, <https://doi.org/10.5194/acp-14-12665-2014>, <https://www.atmos-chem-phys.net/14/12665/2014/>, 2014.
- 10 Grell, G. A.: Prognostic Evaluation of Assumptions Used by Cumulus Parameterizations, *Monthly Weather Review*, 121, 764–787, [https://doi.org/10.1175/1520-0493\(1993\)121<0764:PEOAUB>2.0.CO;2](https://doi.org/10.1175/1520-0493(1993)121<0764:PEOAUB>2.0.CO;2), [https://doi.org/10.1175/1520-0493\(1993\)121<0764:PEOAUB>2.0.CO;2](https://doi.org/10.1175/1520-0493(1993)121<0764:PEOAUB>2.0.CO;2), 1993.
- Grell, G. A. and Dévényi, D.: A generalized approach to parameterizing convection combining ensemble and data assimilation techniques, *Geophysical Research Letters*, 29, 38–1–38–4, <https://doi.org/10.1029/2002GL015311>, <https://agupubs.onlinelibrary.wiley.com/doi/abs/10.1029/2002GL015311>, 2002.
- 15 Guenther, A., Karl, T., Harley, P., Wiedinmyer, C., Palmer, P. I., and Geron, C.: Estimates of global terrestrial isoprene emissions using MEGAN (Model of Emissions of Gases and Aerosols from Nature), *Atmos. Chem. Phys.*, 6, 3181–3210, <https://doi.org/10.5194/acp-6-3181-2006>, <http://www.atmos-chem-phys.net/6/3181/2006/>, 2006.
- Hudman, R. C., Jacob, D. J., Turquety, S., Leibensperger, E. M., Murray, L. T., Wu, S., Gilliland, A. B., Avery, M., Bertram, T. H., Brune, W., Cohen, R. C., Dibb, J. E., Flocke, F. M., Fried, A., Holloway, J., Neuman, J. A., Orville, R., Perring, A., Ren, X., Sachse, G. W., Singh, H. B., Swanson, A., and Wooldridge, P. J.: Surface and lightning sources of nitrogen oxides over the United States: Magnitudes, chemical evolution, and outflow, *J. Geophys. Res. Atmos.*, 112, <https://doi.org/10.1029/2006JD007912>, 2007.
- 20 Huntrieser, H., Schlager, H., Lichtenstern, M., Roiger, A., Stock, P., Minikin, A., Höller, H., Schmidt, K., Betz, H.-D., Allen, G., Viciani, S., Ulanovsky, A., Ravegnani, F., and Brunner, D.: NO_x production by lightning in Hector: first airborne measurements during SCOUT-O3/ACTIVE, *Atmospheric Chemistry and Physics*, 9, 8377–8412, <https://doi.org/10.5194/acp-9-8377-2009>, <https://www.atmos-chem-phys.net/9/8377/2009/>, 2009.
- 25 Jourdain, L., Kulawik, S. S., Worden, H. M., Pickering, K. E., Worden, J., and Thompson, A. M.: Lightning NO_x emissions over the USA constrained by TES ozone observations and the GEOS-Chem model, *Atmospheric Chemistry and Physics*, 10, 107–119, <https://doi.org/10.5194/acp-10-107-2010>, <https://www.atmos-chem-phys.net/10/107/2010/>, 2010.
- 30 Kain, J. S.: The Kain–Fritsch Convective Parameterization: An Update, *Journal of Applied Meteorology*, 43, 170–181, [https://doi.org/10.1175/1520-0450\(2004\)043<0170:TKCPAU>2.0.CO;2](https://doi.org/10.1175/1520-0450(2004)043<0170:TKCPAU>2.0.CO;2), [https://doi.org/10.1175/1520-0450\(2004\)043<0170:TKCPAU>2.0.CO;2](https://doi.org/10.1175/1520-0450(2004)043<0170:TKCPAU>2.0.CO;2), 2004.
- Kain, J. S. and Fritsch, J. M.: A One-Dimensional Entraining/Detraining Plume Model and Its Application in Convective Parameterization, *Journal of the Atmospheric Sciences*, 47, 2784–2802, [https://doi.org/10.1175/1520-0469\(1990\)047<2784:AODEPM>2.0.CO;2](https://doi.org/10.1175/1520-0469(1990)047<2784:AODEPM>2.0.CO;2), [https://doi.org/10.1175/1520-0469\(1990\)047<2784:AODEPM>2.0.CO;2](https://doi.org/10.1175/1520-0469(1990)047<2784:AODEPM>2.0.CO;2), 1990.
- 35 Lamsal, L. N., Martin, R. V., Padmanabhan, A., van Donkelaar, A., Zhang, Q., Sioris, C. E., Chance, K., Kurosu, T. P., and Newchurch, M. J.: Application of satellite observations for timely updates to global anthropogenic NO_x emission inventories, *Geophysical Research Letters*, 38, n/a–n/a, <https://doi.org/10.1029/2010gl046476>, <https://doi.org/10.1029/2010gl046476>, 2011.



- Laughner, J. L. and Cohen, R. C.: Quantification of the effect of modeled lightning NO₂ on UV-visible air mass factors, *Atmos. Meas. Tech. Discuss.*, 2017.
- Laughner, J. L. and Zhu, Q.: CohenBerkeleyLab/BEHR-Core: BEHR Core code, <https://doi.org/10.5f281/zenodo.998275>, 2018.
- Laughner, J. L., Zhu, Q., and Cohen, R. C.: The Berkeley High Resolution Tropospheric NO₂ Product, *Earth System Science Data Discussions*, 2018, 1–33, <https://doi.org/10.5194/essd-2018-66>, <https://www.earth-syst-sci-data-discuss.net/essd-2018-66/>, 2018.
- Laughner, J. L., Zhu, Q., and Cohen, R. C.: Evaluation of version 3.0B of the BEHR OMI NO₂ product, *Atmospheric Measurement Techniques*, 12, 129–146, <https://doi.org/10.5194/amt-12-129-2019>, <https://www.atmos-meas-tech.net/12/129/2019/>, 2019.
- Levelt, P., Oord, G., R. Dobber, M., Mälkki, A., Visser, H., Vries, J., Stammes, P., Lundell, J., and Saari, H.: The Ozone Monitoring Instrument, *IEEE T. Geoscience and Remote Sensing*, 44, 1093–1101, <https://doi.org/10.1109/TGRS.2006.872333>, 2006.
- Liaskos, C. E., Allen, D. J., and Pickering, K. E.: Sensitivity of tropical tropospheric composition to lightning NO_x production as determined by replay simulations with GEOS-5, *Journal of Geophysical Research: Atmospheres*, 120, 8512–8534, <https://doi.org/10.1002/2014JD022987>, <https://agupubs.onlinelibrary.wiley.com/doi/abs/10.1002/2014JD022987>, 2015.
- Lu, Z., Streets, D. G., de Foy, B., Lamsal, L. N., Duncan, B. N., and Xing, J.: Emissions of nitrogen oxides from US urban areas: estimation from Ozone Monitoring Instrument retrievals for 2005–2014, *Atmospheric Chemistry and Physics*, 15, 10367–10383, <https://doi.org/10.5194/acp-15-10367-2015>, <https://www.atmos-chem-phys.net/15/10367/2015/>, 2015.
- Luo, C., Wang, Y., and Koshak, W. J.: Development of a self-consistent lightning NO_x simulation in large-scale 3-D models, *Journal of Geophysical Research: Atmospheres*, 122, 3141–3154, <https://doi.org/10.1002/2016JD026225>, <https://agupubs.onlinelibrary.wiley.com/doi/abs/10.1002/2016JD026225>, 2017.
- Mak, H. W. L., Laughner, J. L., Fung, J. C. H., Zhu, Q., and Cohen, R. C.: Improved Satellite Retrieval of Tropospheric NO₂ Column Density via Updating of Air Mass Factor (AMF): Case Study of Southern China, *Remote Sensing*, 10, <http://www.mdpi.com/2072-4292/10/11/1789>, 2018.
- Martin, R., Sauvage, B., Folkens, I., Sioris, C., Boone, C., Bernath, P., and Ziemke, J.: Space-based constraints on the production of nitric oxide by lightning, *J. Geophys. Res. Atmos.*, 112, <https://doi.org/10.1029/2006JD007831>, 2007.
- Miyazaki, K., Eskes, H., and Sudo, K.: Global NO_x emissions estimates derived from an assimilation of OMI tropospheric NO₂ columns, *Atmos. Chem. Phys.*, 12, 2263–2288, <https://doi.org/10.5194/acp-12-2263-2012>, 2012.
- Miyazaki, K., Eskes, H., Sudo, K., and Zhang, C.: Global lightning NO_x production estimated by an assimilation of multiple satellite data sets, *Atmos. Chem. Phys.*, 14, 3277–3305, <https://doi.org/10.5194/acp-14-3277-2014>, 2014.
- Nault, B. A., Laughner, J. L., Wooldridge, P. J., Crouse, J. D., Dibb, J., Diskin, G., Peischl, J., Podolske, J. R., Pollack, I. B., Ryerson, T. B., Scheuer, E., Wennberg, P. O., and Cohen, R. C.: Lightning NO_x Emissions: Reconciling Measured and Modeled Estimates With Updated NO_x Chemistry, *Geophys. Res. Lett.*, <https://doi.org/10.1002/2017GL074436>, 2017.
- Ott, L. E., Pickering, K. E., Stenchikov, G. L., Allen, D. J., DeCaria, A. J., Ridley, B., Lin, R.-F., Lang, S., and Tao, W.-K.: Production of lightning NO_x and its vertical distribution calculated from three-dimensional cloud-scale chemical transport model simulations, *Journal of Geophysical Research*, 115, <https://doi.org/10.1029/2009jd011880>, <https://doi.org/10.1029/2009jd011880>, 2010.
- Pickering, K. E., Bucsela, E., Allen, D., Ring, A., Holzworth, R., and Krotkov, N.: Estimates of lightning NO_x production based on OMI NO₂ observations over the Gulf of Mexico, *J. Geophys. Res. Atmos.*, 121, 8668–8691, <https://doi.org/10.1002/2015JD024179>, <http://dx.doi.org/10.1002/2015JD024179>, 2015JD024179, 2016.
- Pollack, I. B., Homeyer, C. R., Ryerson, T. B., Aikin, K. C., Peischl, J., Apel, E. C., Campos, T., Flocke, F., Hornbrook, R. S., Knapp, D. J., Montzka, D. D., Weinheimer, A. J., Riemer, D., Diskin, G., Sachse, G., Mikoviny, T., Wisthaler, A., Bruning, E., MacGorman, D.,



- Cummings, K. A., Pickering, K. E., Huntrieser, H., Lichtenstern, M., Schlager, H., and Barth, M. C.: Airborne quantification of upper tropospheric NO_x production from lightning in deep convective storms over the United States Great Plains, *Journal of Geophysical Research: Atmospheres*, 121, 2002–2028, <https://doi.org/10.1002/2015JD023941>, <https://agupubs.onlinelibrary.wiley.com/doi/abs/10.1002/2015JD023941>, 2016.
- 5 Price, C. and Rind, D.: A simple lightning parameterization for calculating global lightning distributions, *Journal of Geophysical Research: Atmospheres*, 97, 9919–9933, <https://doi.org/10.1029/92JD00719>, <https://agupubs.onlinelibrary.wiley.com/doi/abs/10.1029/92JD00719>, 1992.
- Price, C., Penner, J., and Prather, M.: NO_x from lightning: 1. Global distribution based on lightning physics, *Journal of Geophysical Research: Atmospheres*, 102, 5929–5941, <https://doi.org/10.1029/96JD03504>, <https://agupubs.onlinelibrary.wiley.com/doi/abs/10.1029/96JD03504>,
10 1997.
- Romps, D. M., Seeley, J. T., Vollaro, D., and Molinari, J.: Projected increase in lightning strikes in the United States due to global warming, *Science*, 346, 851–854, <https://doi.org/10.1126/science.1259100>, <http://science.sciencemag.org/content/346/6211/851>, 2014.
- Rudlosky, S. D.: Evaluating ENTLN Performance Relative to TRMM/LIS., *Journal of Operational Meteorology*, 3, 2015.
- Russell, A. R., Valin, L. C., and Cohen, R. C.: Trends in OMI NO₂ observations over the United States: effects of emission control technology
15 and the economic recession, *Atmos. Chem. Phys.*, 12, 12 197–12 209, <https://doi.org/10.5194/acp-12-12197-2012>, 2012.
- Schumann, U. and Huntrieser, H.: The global lightning-induced nitrogen oxides source, *Atmospheric Chemistry and Physics*, 7, 3823–3907, <https://doi.org/10.5194/acp-7-3823-2007>, <https://www.atmos-chem-phys.net/7/3823/2007/>, 2007.
- Silvern, R. F., Jacob, D. J., Travis, K. R., Sherwen, T., Evans, M. J., Cohen, R. C., Laughner, J. L., Hall, S. R., Ullmann, K., Crouse, J. D.,
Wennberg, P. O., Peischl, J., and Pollack, I. B.: Observed NO/NO₂ Ratios in the Upper Troposphere Imply Errors in NO-NO₂-O₃ Cycling
20 Kinetics or an Unaccounted NO_x Reservoir, *Geophysical Research Letters*, 45, 4466–4474, <https://doi.org/10.1029/2018GL077728>, <https://agupubs.onlinelibrary.wiley.com/doi/abs/10.1029/2018GL077728>, 2018.
- Tippett, M. K. and Koshak, W. J.: A Baseline for the Predictability of U.S. Cloud-to-Ground Lightning, *Geophysical Research Letters*, 0, <https://doi.org/10.1029/2018GL079750>, <https://agupubs.onlinelibrary.wiley.com/doi/abs/10.1029/2018GL079750>, 2018.
- Toon, O. B., Maring, H., Dibb, J., Ferrare, R., Jacob, D. J., Jensen, E. J., Luo, Z. J., Mace, G. G., Pan, L. L., Pfister, L., Rosenlof, K. H., Redemann, J., Reid, J. S., Singh, H. B., Thompson, A. M., Yokelson, R., Minnis, P., Chen, G., Jucks, K. W., and Pszenny, A.: Planning, implementation, and scientific goals of the Studies of Emissions and Atmospheric Composition, Clouds and Climate Coupling by Regional Surveys (SEAC4RS) field mission, *Journal of Geophysical Research: Atmospheres*, 121, 4967–5009, <https://doi.org/10.1002/2015JD024297>, <https://agupubs.onlinelibrary.wiley.com/doi/abs/10.1002/2015JD024297>, 2016.
- Tost, H., Jöckel, P., and Lelieveld, J.: Lightning and convection parameterisations; uncertainties in global modelling, *Atmospheric Chemistry and Physics*, 7, 4553–4568, <https://doi.org/10.5194/acp-7-4553-2007>, <https://www.atmos-chem-phys.net/7/4553/2007/>, 2007.
- Travis, K. R., Jacob, D. J., Fisher, J. A., Kim, P. S., Marais, E. A., Zhu, L., Yu, K., Miller, C. C., Yantosca, R. M., Sulprizio, M. P., Thompson, A. M., Wennberg, P. O., Crouse, J. D., St. Clair, J. M., Cohen, R. C., Laughner, J. L., Dibb, J. E., Hall, S. R., Ullmann, K., Wolfe, G. M., Pollack, I. B., Peischl, J., Neuman, J. A., and Zhou, X.: Why do models overestimate surface ozone in the Southeast United States?, *Atmos. Chem. Phys.*, 16, 13 561–13 577, <https://doi.org/10.5194/acp-16-13561-2016>, <https://www.atmos-chem-phys.net/16/13561/2016/>, 2016.
- 35 Wong, J., Barth, M. C., and Noone, D.: Evaluating a lightning parameterization based on cloud-top height for mesoscale numerical model simulations, *Geoscientific Model Development*, 6, 429–443, <https://doi.org/10.5194/gmd-6-429-2013>, <https://www.geosci-model-dev.net/6/429/2013/>, 2013.



- Zare, A., Romer, P. S., Nguyen, T., Keutsch, F. N., Skog, K., and Cohen, R. C.: A comprehensive organic nitrate chemistry: insights into the lifetime of atmospheric organic nitrates, *Atmospheric Chemistry and Physics*, 18, 15 419–15 436, <https://doi.org/10.5194/acp-18-15419-2018>, <https://www.atmos-chem-phys.net/18/15419/2018/>, 2018.
- Zhao, C., Wang, Y., Choi, Y., and Zeng, T.: Summertime impact of convective transport and lightning NO_x production over North America: modeling dependence on meteorological simulations, *Atmospheric Chemistry and Physics*, 9, 4315–4327, <https://doi.org/10.5194/acp-9-4315-2009>, <https://www.atmos-chem-phys.net/9/4315/2009/>, 2009.
- Zhu, Q. and Laughner, J. L.: CohenBerkeleyLab/WRF-Chem-R2SMH: WRF-Chem code, <https://doi.org/10.5281/zenodo.2585381>, 2019.
- Zhu, Q., Laughner, J., and Cohen, R.: Berkeley High Resolution (BEHR) OMI NO_2 v3.0C - Gridded pixels, daily profiles, v3, UC Berkeley Dash, Dataset, <https://doi.org/10.6078/D16X1T>, 2019a.
- 10 Zhu, Q., Laughner, J., and Cohen, R.: Berkeley High Resolution (BEHR) OMI NO_2 v3.0C - Native pixels, daily profiles, UC Berkeley Dash, Dataset, <https://doi.org/10.6078/D1BM2B>, 2019b.